DEVELOPMENT MODEL OF A HIGH-PERFORMANCE MULTIPLE INPUT MULTIPLE OUTPUT MICROSTRIP ANTENNA BASED ON A PLANAR SERIES ARRAY WITH 8×2 ELEMENTS FOR 5G COMMUNICATION SYSTEMS

MIMO (Multiple Input Multiple Output) makes a major contribution to 5G communication systems by increasing network capacity and spectrum efficiency. In 5G, MIMO enables the use of multiple antennas at base stations and user devices, allowing simultaneous sending and receiving of data over multiple paths. This significantly increases data throughput and connection reliability, especially in environments with high user density. In addition, MIMO technology supports the implementation of beamforming, which focuses signals on a specific direction, reduces interference, and improves signal coverage and quality, making it one of the keys to achieving faster and more responsive 5G performance. Therefore, antennas with wide bandwidth, high gain and MIMO performance are crucial for supporting 5G communication systems. This paper proposes a high-performance MIMO microstrip antenna based on a series planar array with 8×2 elements operating at a resonant frequency of 3.5 GHz for 5G communication systems. A spiral stub and a feed inset are proposed to control the reflection coefficient and bandwidth of the antenna while the series planar array is proposed to increase the gain. To support the MIMO communication system, the proposed antenna is separated into two different ports with a certain distance. From the measurement results, the proposed antenna has high performance indicated by a wide bandwidth of 680 MHz (3–3.68 GHz) and a high gain of 17.8 dB at a resonant frequency of 3.5 GHz. In addition, the proposed antenna has high mutual coupling and diversity indicated by ECC and DG of 0.001 and 9.99 dB, respectively. This work provides a solution to design a high-performance microstrip antenna and can be implemented as a receiving antenna for 5G communication systems

Keywords: microstrip antenna, high gain, MIMO system, planar array, 5G system

Syah Alam
Corresponding author
Doctor of Electrical Engineering, Associate Professor, Lecture*
E-mail: syah.alam@trisakti.ac.id
Indra Surjati
Doctor of Electrical Engineering, Professor, Lecture*
Lydia Sari
Doctor of Electrical Engineering, Associate Professor, Lecture*
Yuli Kurnia Ningsih
Doctor of Electrical Enginnering, Associate Professor, Lecture*
Suryadi Suryadi
Bachelor of Electrical Enginnering, Assistant Professor, Lecture*
Teguh Firmansyah
Doctor of Electrical Engineering, Lecturer
Department of Electrical Engineering
Universitas Sultan Ageng Tirtayasa
Ciwaru Raya str., 25, Serang, Banten, Indonesia, 42117
Zahriladha Zakaria
Doctor of Electrical Engineering, Professor
Faculty of Electronic Engineering and Computer Engineering (FKEKK)
Universiti Teknikal Malaysia Melaka (UTeM)
Hang Tuah Jaya str., Durian Tunggal, Melaka, Malaysia, 76100
*Department of Electrical Engineering
Universitas Trisakti
Kyai Tapa str., 1, DKI Jakarta, Indonesia, 11440

1. Introduction

5G communication systems require more sophisticated and diverse antennas than previous generations to support various technological advancements, such as MIMO and millimeter wave (mmWave) [1–3]. MIMO (Multiple Input Multiple Output) is a technology that plays a key role in 5G communication systems. The main advantage of MIMO in 5G is its ability to significantly increase capacity and data rates without requiring more frequency spectrum. By using multiple antennas on the transmit and receive side, MIMO allows simultaneous data transmission over multiple paths, reducing interference and increasing spectral efficiency [4, 5]. In addition, MIMO can improve signal coverage and reliability by using techniques such as beamforming, which focuses the signal toward a specific user. This is especially important in delivering a faster and more stable experience for users in sub-urban areas [6]. According to [7], the resonant frequency for 5G communication systems is categorized into three bands: high, middle, and low. One of the recommended

frequencies for 5G communication systems is 3.5 GHz, which is included in the middle band category and dynamic environments, such as urban or high-mobility areas [8].

Furthermore, microstrip antennas offer several important advantages for 5G applications, particularly in terms of integration, size, and performance [9, 10]. Due to their thin and lightweight design, microstrip antennas can be easily integrated into portable devices such as smartphones and IoT devices, as well as into network infrastructure such as base stations [11, 12]. They can also be manufactured in arrays, enabling the implementation of MIMO and beamforming technologies, which are essential for increasing the capacity and transmission speed in 5G networks [13, 14]. In addition, microstrip antennas can be designed to operate at a wide range of frequencies, including high frequencies such as mmWave used in 5G, while maintaining good efficiency. Their relatively low production costs and ability to be printed on a variety of substrates also make them an economical and practical choice for widespread 5G deployment. However, microstrip antennas have certain drawbacks, such as narrow bandwidth, low gain, and limited directivity. The primary parameters that indicate an antenna's performance include the reflection coefficient, bandwidth, gain, and radiation pattern. Therefore, antennas with wide bandwidth and high gain are crucial for supporting wireless communication systems such as Wi-Fi, 4G, and 5G. Moreover, high-performance antennas with multiple input multiple output are essential to facilitate communication between the transmitter and receiver, especially for 5G communication systems.

2. Literature review and problem statement

Several previous studies have explored and proposed microstrip antennas for 5G communication systems using various techniques, including fractal designs, arrays, and parasitic elements. Furthermore, in a study presented by [10], microstrip antennas with wider bandwidths were achieved by incorporating parasitic elements placed above the radiating elements. However, the antenna's gain remained low, necessitating further improvement. Previous work [15] proposed a fractal antenna for 5G communication with MIMO configuration operating at a resonant frequency of 3.5 GHz. However, the gain of the proposed antenna is still low at about 3 dB. Another work [16] proposed a ten-element MIMO array antenna that operates at a resonant frequency of 3.5 GHz. However, the bandwidth of the proposed antenna is still low at about 200 MHz. Moreover, the previous work [17] presented a wideband microstrip antenna operating at a resonant frequency of 3.35–3.95 GHz with a 2×2 element MIMO array. However, the gain of the proposed antenna is only 12.6 dB. Another study by [18] proposed a microstrip antenna array with four elements operating at a resonant frequency of 3.5 GHz, achieving a bandwidth of 0.7 GHz and a gain of 9.24 dB. Nevertheless, the increase in bandwidth was accompanied by a decrease in gain, indicating an inverse relationship between bandwidth and gain. In addition, previous work by [19] proposed a microstrip antenna using an array with 4×2 elements with a bandwidth of 0.6 GHz and a gain of 12.2 dB. However, the proposed antenna does not support MIMO communication systems. Other findings describe MIMO microstrip antennas based on vertical and horizontal configurations with 2 ports operating at resonant frequencies of 3.5 GHz and 6 GHz [20].

However, the gain obtained is still low at around 7.8 dB. Based on the literature review [15–20], the limitation of previous works is that the proposed antenna still has low gain, narrow bandwidth and does not support MIMO. Therefore, an antenna with wide bandwidth, high gain and MIMO support is needed as a solution for receivers in 5G communication systems. In addition, MIMO technology supports the implementation of beamforming, which focuses signals on a specific direction, reduces interference, and improves signal coverage and quality, making it one of the keys to achieving faster and more responsive 5G performance.

3. The aim and objectives of the study

The aim of the study is to propose an antenna configured with two different ports separated by a certain distance in order to support MIMO capabilities.

To achieve this aim, the following objectives are accomplished:

– to produce a design and model of a microstrip antenna that operates at a resonance frequency of 3.5 GHz with a bandwidth of 200 MHz for a 5G communication system;

– to produce a design and model of a microstrip antenna with a high gain ≥12 dB that operates at a frequency of 3.5 GHz for a 5G communication system;

– to validate and measure microstrip antennas that can be used in MIMO communication systems with low mutual coupling $S_{21} \leq -20$ dB.

4. Materials and methods

The object of the study is 5G communication systems. The main hypothesis of the study is as follows. A high-performance MIMO microstrip antenna based on a series planar array with 8x2 elements operating at a resonant frequency of 3.5 GHz, will improve the capabilities of 5G communication systems.

The proposed antenna is designed using an FR-4 substrate with a dielectric constant of 4.3, tan delta of 0.0265 and thickness of 1.6 mm. The radiation element of the antenna is represented by a rectangular patch placed on the top layer of the substrate while the bottom layer functions as a ground plane. The antenna is connected directly with a brass connector using a microstrip line with an impedance of 50 ohms. The evolution and models of the proposed antenna are shown in Fig. 1. The antenna is designed and simulated using EM simulation based on HFSS 15.0.

Fig. 1 shows that the proposed antenna is developed in six models. Model 1 proposes an antenna with a single element that operates at a resonance frequency of 3.5 GHz, which is represented in Fig. 1, a. Furthermore, model 2 and model 3 propose two-element and four-element array antennas based on a series configuration with a spiral stub shown in Fig. 1, b, c.

Model 4 proposes an eight-element array antenna by adding an inset fed to the antenna patch while model 5 proposes an array antenna with 8×2 elements configured based on the horizontal planar shown in Fig. 1, d, e. The last model proposes an array antenna with 8×2 elements configured as MIMO using two ports separated by a certain distance represented by Fig. 1, f. The addition of the spiral stub and fed inset aims to reduce the reflection coefficient while adding the number of elements on the array antenna aims to increase the gain.
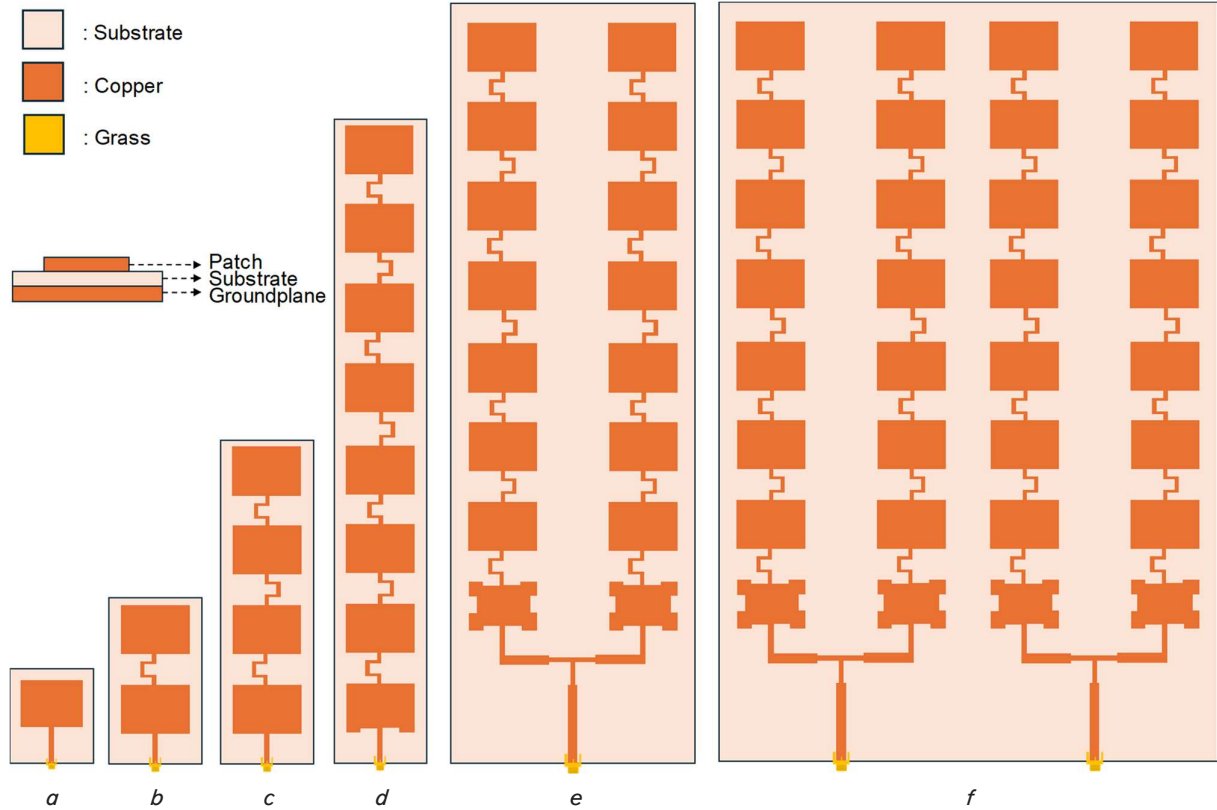
Fig. 1. Evolution of the proposed antenna: *a* — single-element; *b* — 2-element array; *c* — 4-element array; *d* — 8-element array; *e* — 8×2 element planar array; *f* — MIMO planar array

5. Results of the design and realization of the proposed antenna

5. 1. Design of a series array antenna

At the first stage, the antenna is designed with a rectangular patch to operate at a resonant frequency of 3.5 GHz. The length and width of the antenna patch are represented respectively by W_p and L_p, which are determined based on the following equation [21]:

$$W_p = \frac{c}{2f_o\sqrt{\frac{\varepsilon_r}{2}}},$$ (1)

$$L_p = L_{eff} - \Delta_L,$$ (2)

$$L_{eff} = \frac{c}{2f_o\sqrt{\varepsilon_{eff}}},$$ (3)

$$\varepsilon_{eff} = \frac{\varepsilon r + 1}{2} + \frac{\varepsilon r - 1}{2}\left[1 + 12\frac{h}{W}\right]^{-\frac{1}{2}},$$ (4)

$$\Delta_L = 0.412\frac{\left(\varepsilon_{reff} + 0.3\right)\left(\frac{W}{h} + 0.264\right)}{\left(\varepsilon_{reff} - 0.258\right)\left(\frac{W}{h} + 0.8\right)}.$$ (5)

In this context, W_p and L_p denote the width and length of the patch, respectively; f_o signifies the resonance frequency, ε_r indicates the substrate's permittivity, ε_{eff} refers to the effective permittivity of the substrate at a specific resonance frequency, h stands for the substrate's thickness, and Δ_L

accounts for the fringing field's edge effect on the patch. In addition, microstrip lines are suggested for managing the impedance and reflection coefficient of the antenna. The size of the microstrip line is significantly affected by the input impedance and the chosen resonant frequency. In this study, the input impedance is set to 50 ohms. The dimensions of the microstrip line can be calculated using the following equation [22]:

$$W_z = \frac{2h}{\pi}\left\{B - 1 - \ln\left(2B - 1\right) + \frac{\varepsilon_r - 1}{2\varepsilon_r}\left[\ln\left(B - 1\right) + 0.39 - \frac{0.61}{\varepsilon_r}\right]\right\},$$ (6)

$$B = \frac{60\pi^2}{Z_0\sqrt{\varepsilon_{eff}}}.$$ (7)

In this context, W_z represents the width of the microstrip line, π is constant, Z_o denotes the antenna's impedance, and B stands for the impedance constant. The antenna's impedance is 50 Ω, matching the impedance of the connector used. Additionally, the length of the microstrip line (L_z) is ¼ of the wavelength (λ_g), calculated using the following equation [21]:

$$L_z = \frac{1}{4}\lambda_g,$$ (8)

$$\lambda_g = \frac{\lambda}{\varepsilon_{eff}}.$$ (9)

The structure and simulation results of an antenna with a single element are shown in Fig. 2.
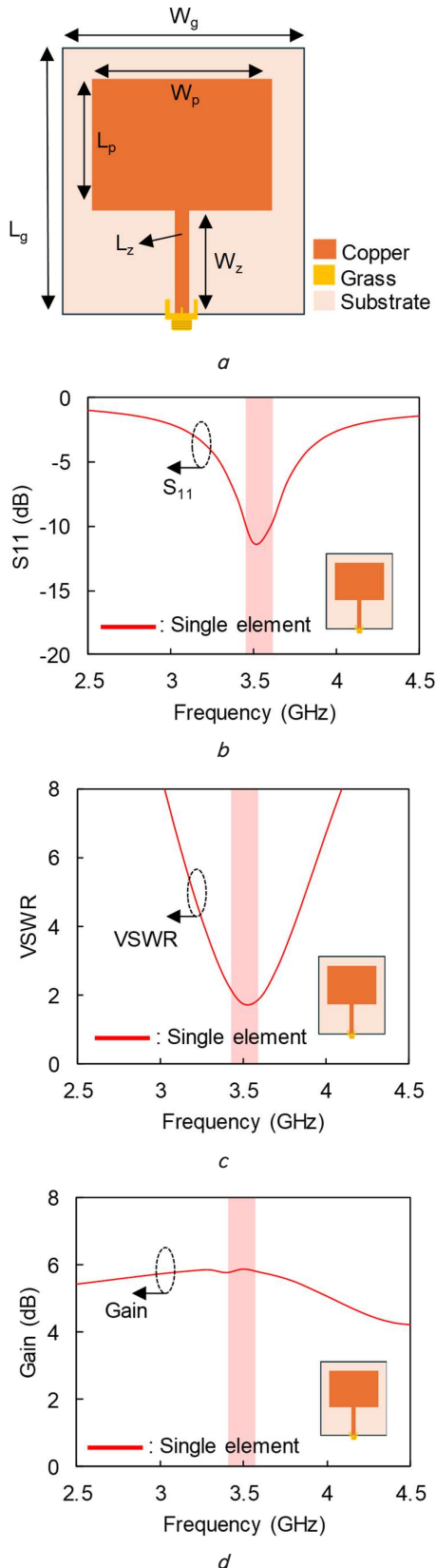
Fig. 2. Model of a single-element antenna: *a* — design of a single element; *b* — simulation of S_{11}; *c* — simulation of VSWR; *d* — simulation of gain

Fig. 2, *a* shows the dimensions of W_p and L_p being 26 mm and 22 mm, respectively. In addition, the length and width of the microstrip lines represented by L_z and W_z are

13 mm and 3 mm. The dimensions of the ground plane are shown by W_g and L_g where the width and length are 35 mm and 29 mm. Furthermore, the simulation results of S_{11}, VSWR in Fig. 2, *a*, *b* show that the antenna has been operating at a resonance frequency of 3.5 GHz with S_{11} –11.34 dB and VSWR 1.74. The gain of the single-element antenna is shown in Fig. 2, *c* where the peak gain at a resonance frequency of 3.5 GHz is 5.8 dB. However, the bandwidth obtained from the single-element antenna is still narrow at 40 MHz (3.48–3.52 GHz). Therefore, optimization is required to increase the bandwidth of the proposed antenna.

The second stage is to optimize the single-element antenna into a series array antenna with two elements. The purpose of adding elements is to increase the gain while the bandwidth of the antenna is optimized with a spiral-shaped stub. The structure and simulation results of an array antenna with two elements are shown in Fig. 3.

Fig. 3, *a* shows the structure of an array antenna with two elements, where the dimensions of W_g and L_g are 32 mm and 71 mm. Moreover, spiral stubs are proposed to connect between elements with lengths L_1, L_2 and L_3 of 6 mm, 7 mm and 6 mm. Furthermore, the width of the spiral stub is represented by W_b and W_s where the width is 3 mm and 1 mm, respectively. The simulation results of S_{11} and VSWR for an array antenna with two elements are shown in Fig. 3, *b*, *c* where S_{11} is –16.79 dB and VSWR is 1.33 at a resonance frequency of 3.5 GHz. The bandwidth obtained from the antenna array with two elements is 400 MHz (3.2–3.6 GHz) with a peak gain of 7.82 dB. This finding shows that the spiral stub and the addition of elements succeed in increasing the bandwidth and gain of the proposed antenna. However, the gain obtained is still low so further optimization is required. Therefore, the gain of the proposed antenna is optimized by increasing the number of elements of the array.

The third stage is to increase the antenna gain by optimizing the antenna array into four elements. The structure and simulation results of an array antenna with four elements are shown in Fig. 4.

Fig. 4, *a* illustrates the design of a four-element array antenna, with W_g and L_g of 32 mm and 142 mm, respectively. The array elements are linked by spiral stubs that extend in opposite directions. Furthermore, the simulation of S_{11} and VSWR shows that the antenna has high performance with S_{11} and VSWR of –29.28 dB and 1.07 at a resonance frequency of 3.5 GHz as shown in Fig. 4, *b*, *c*. The bandwidth obtained from the antenna array with four elements is 300 MHz (3.3–3.6 GHz) with a peak gain of 9.9 dB at a resonance frequency of 3.5 GHz as illustrated in Fig. 4, *d*.

The fourth stage is to optimize the antenna array with eight elements to increase the gain. Furthermore, an inset feed is proposed to control the resonant frequency of the antenna represented by W_i and W_d with dimensions of 7 mm and 1 mm, respectively. The length and width of the ground plane represented by W_g and L_g are 32 mm and 310 mm as shown in Fig. 5, *a*.

The simulation of S_{11} and VSWR of the array antenna with eight elements illustrated in Fig. 5, *b*, *c* shows that the antenna has been operating at a resonance frequency of 3.5 GHz with S_{11} of –26.37 dB and VSWR of 1.10. The bandwidth obtained is 300 MHz (3.3–3.6 GHz) while the peak gain is 10.82 dB at a resonance frequency of 3.5 GHz as shown in Fig. 5, *d*. Furthermore, the simulation results of S_{11} and the gain of the entire antenna model shown in Fig. 6, *a*, *b* are proposed to evaluate the optimization of the proposed antenna, respectively.
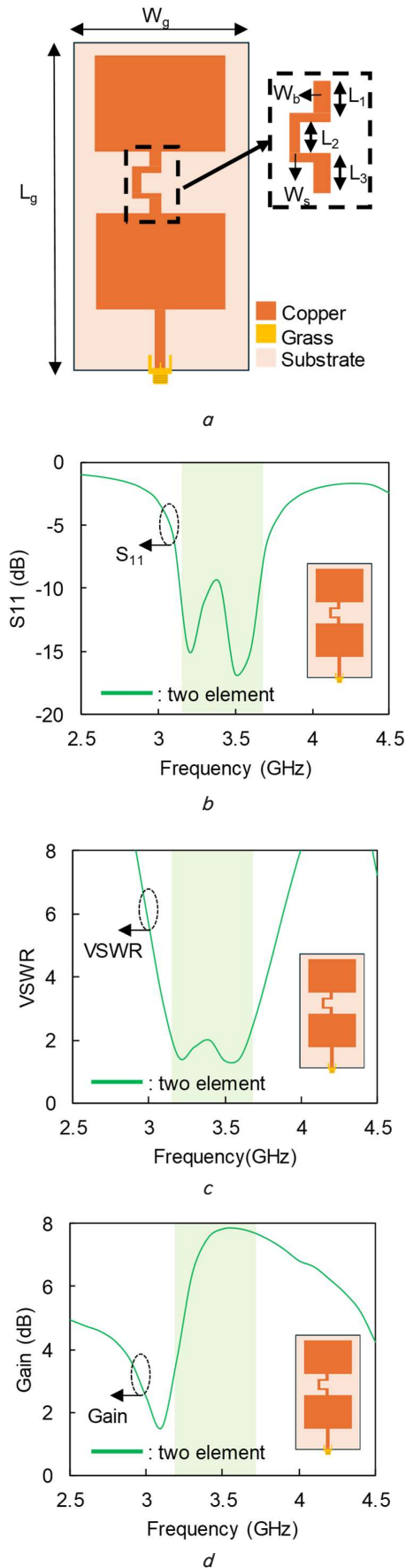
a

b

c

d

Fig. 3. Model of an array antenna with two elements: *a* — design of a two-element array with a spiral stub; *b* — simulation of S_{11}; *c* — simulation of VSWR; *d* — simulation of gain
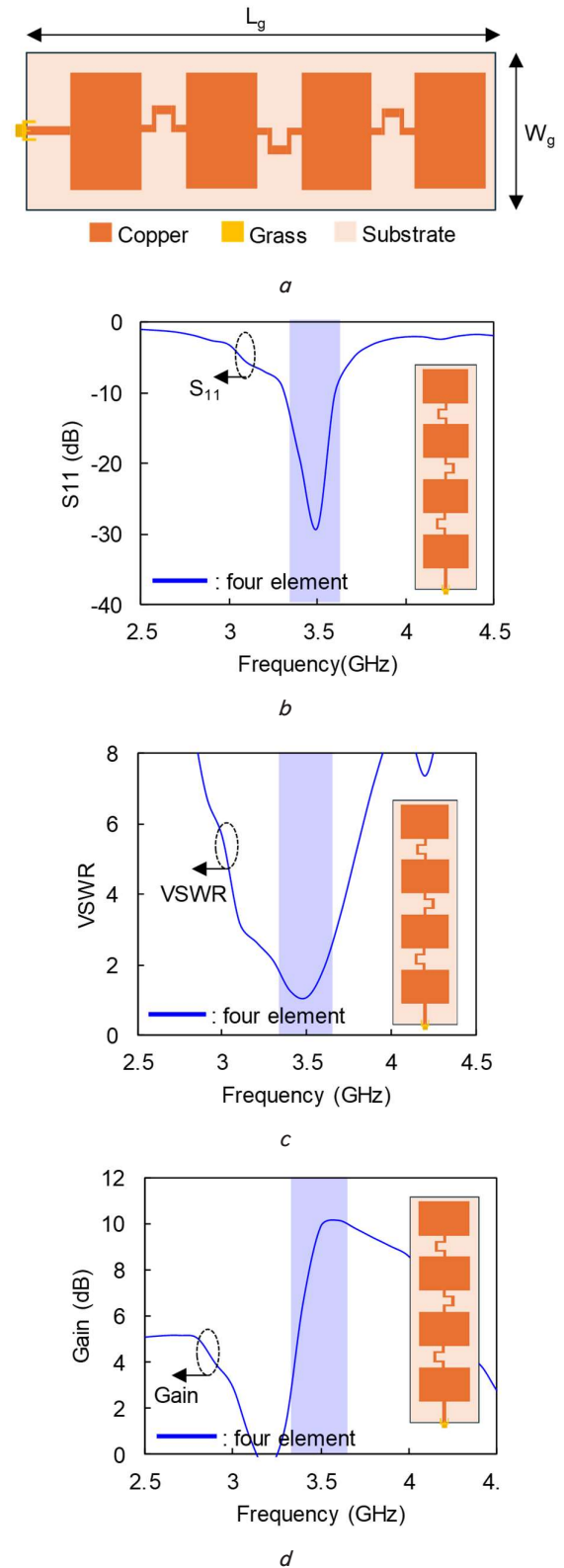

a

b

c

d

Fig. 4. Model of an array antenna with four elements: *a* — design of a four-element array with a spiral stub; *b* — simulation of S_{11}; *c* — simulation of VSWR; *d* — simulation of gain

Fig. 6, *a* illustrates that the reflection coefficient of the proposed antenna gradually improves from −11.23 dB to −26.27 dB at a resonance frequency of 3.5 GHz. This result indicates that the optimization using an eight-element array antenna, spiral stub, and inset feed effectively enhanced the

antenna's performance in terms of the reflection coefficient by up to 134 % compared to a single-element antenna.
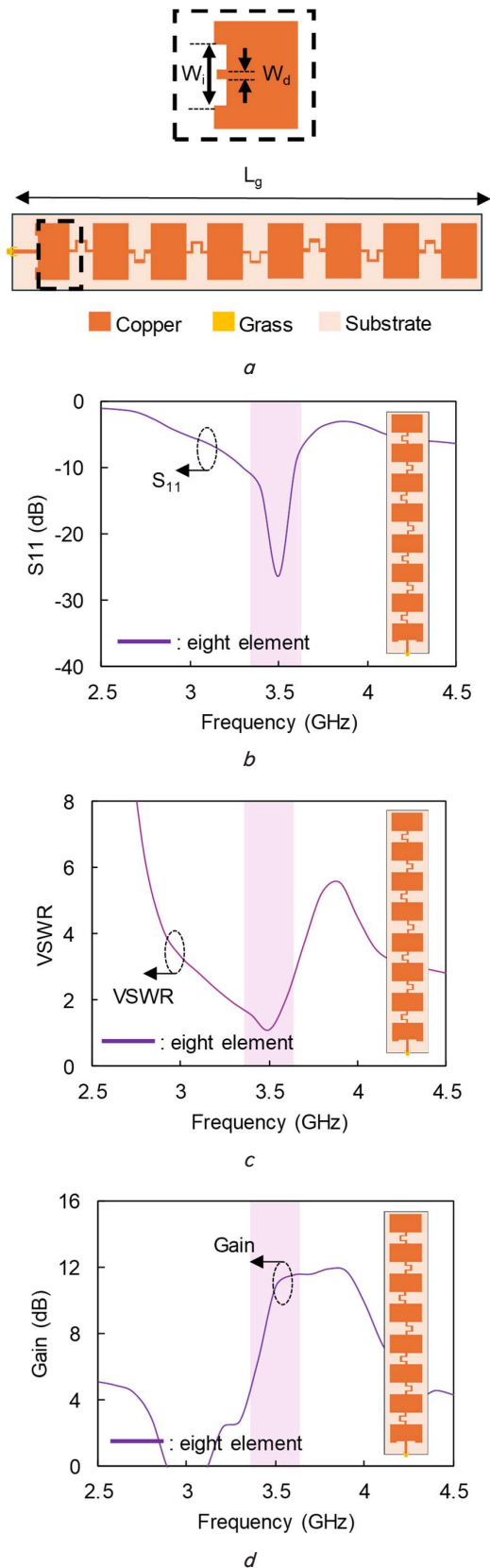

Fig. 5. Model of an array antenna with eight elements: *a* — design of an eight-element array with a spiral stub and inset fed; *b* — simulation of S_{11}; *c* — simulation of VSWR; *d* — simulation of gain
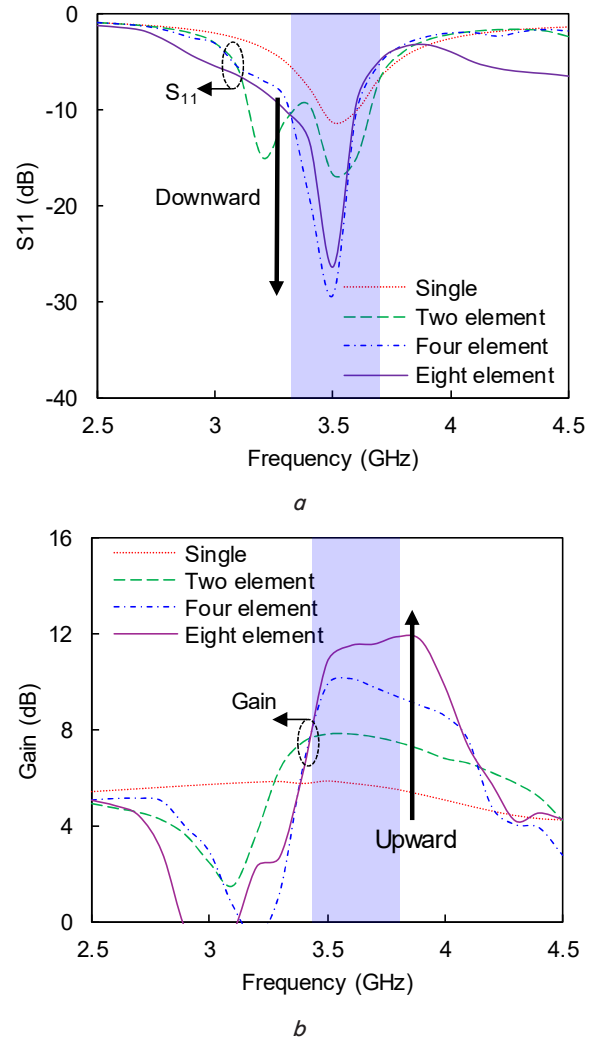

Fig. 6. Comparison of simulation results: *a* — simulation of S_{11}; *b* — simulation of gain

Additionally, the bandwidth of the proposed antenna expanded by 650 %, from 40 MHz (3.48–3.52 GHz) to 300 MHz (3.3–3.6 GHz). This demonstrates that the proposed antenna meets the specifications for the 5G communication system operating within the 3.4–3.6 GHz frequency range. Moreover, Fig. 6, *b* shows that the antenna's gain increases as the number of elements in the antenna array is increased, with a gain improvement of 78 % from 5.8 dB to 10.82 dB at a resonance frequency of 3.5 GHz.

However, the gain of the proposed antenna remains below the desired target ≥12 dB. Thus, additional optimization is necessary to enhance the antenna's gain.

5. 2. Design of a MIMO series planar array antenna with 8x2 elements

In order to increase the gain, the antenna is configured as a series planar array with 8×2 elements. The elements of the antenna array are connected with impedance matching based on T-stubs while the antenna elements are optimized with slits on the right and left edges of the patch. The structure of the series planar array antenna and the simulation results are shown in Fig. 7.

Fig. 7, *a* shows the elements of the antenna separated by a certain distance represented by d_a=21 mm, which is determined based on the following equation [22]:

$$d_a = \frac{1}{8}\lambda, \tag{10}$$

$$\lambda = \frac{c}{f}, \tag{11}$$

where d_a is the distance between elements, λ is the wavelength of the antenna and c is the speed of light $(3 \times 10^8$ m/s). It should be noted that the distance between the ele-

ments of a planar array antenna greatly affects the gain. Furthermore, microstrip lines with stepped impedance are used as impedance matching between elements of the antenna array represented by $Z_1 = 50\ \Omega$, $Z_2 = 70.7\ \Omega$ and $Z_3 = 100\ \Omega$. The width of the transmission line dictates its impedance, which can be calculated using the following equation [21]:
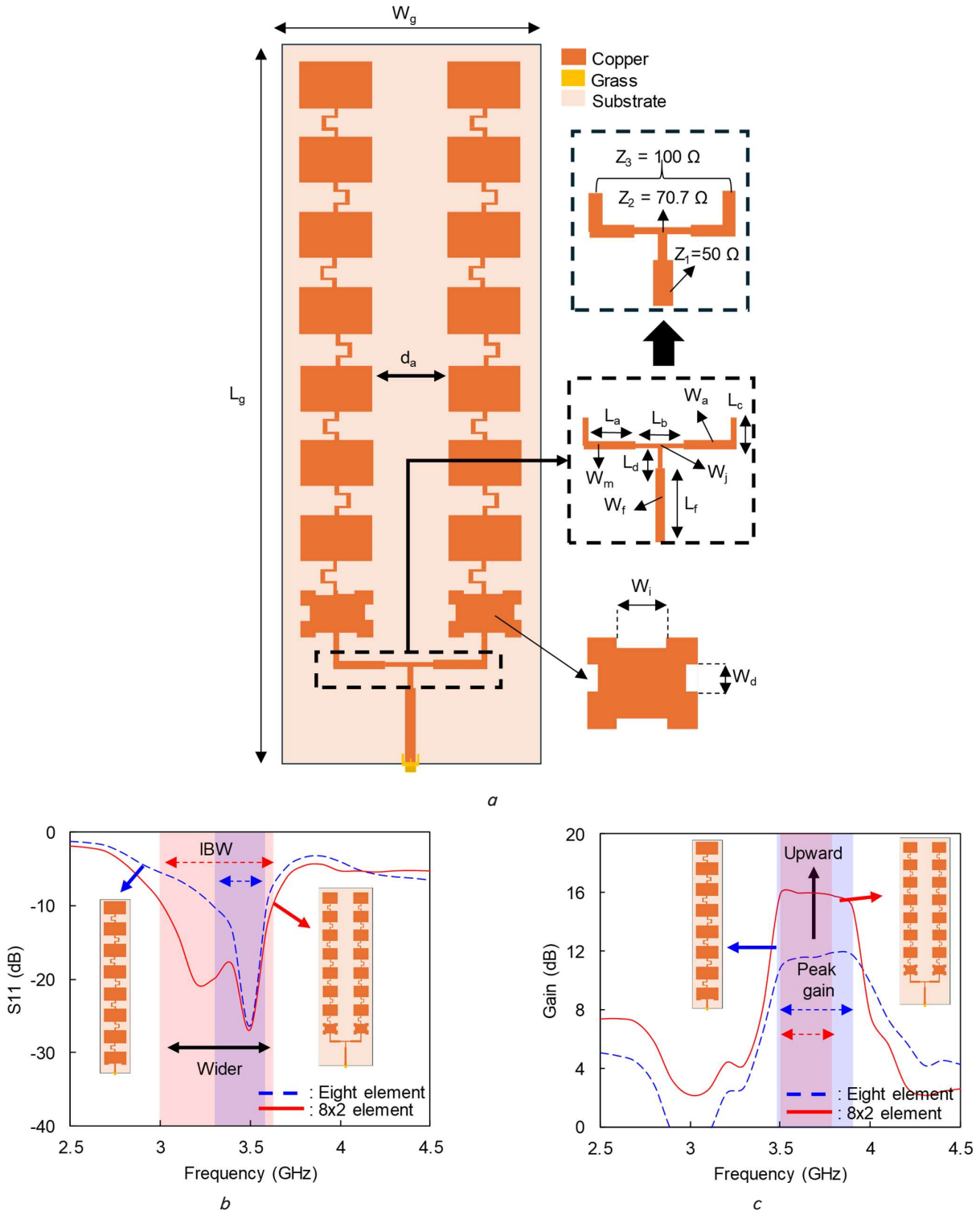
$$Z_2 = \sqrt{Z_1 \cdot Z_3}. \tag{11}$$

Fig. 7. Model of a series planar array antenna: *a* — design of an 8×2 element planar array with a spiral stub and inset fed; *b* — simulation of S_{11}; *c* — simulation of VSWR; *d* — simulation of gain

The width of the microstrip line with stepped imped-ance is represented by W_f=3 mm, W_j=1 mm and W_m=2 mm while the length is represented by L_f=33 mm, L_d=8 mm, L_b=23 mm, L_a=12 mm and L_c=17 mm. The dimensions of the ground plane indicated by W_g and L_g are 82 mm and 353 mm, respectively. Furthermore, Fig. 7, b shows that the bandwidth of the proposed antenna increases from

300 MHz (3.3–3.6 GHz) to 600 MHz (3–3.6 GHz). In ad-dition, the peak gain of the antenna also increases from 10.82 to 16.09 dB at a resonant frequency of 3.5 GHz as shown in Fig. 7, c. These findings indicate that the proposed antenna has met the specifications for a 5G communication system with a bandwidth of ≤200 MHz and a gain of ≥12 dB at a resonant frequency of 3.5 GHz.
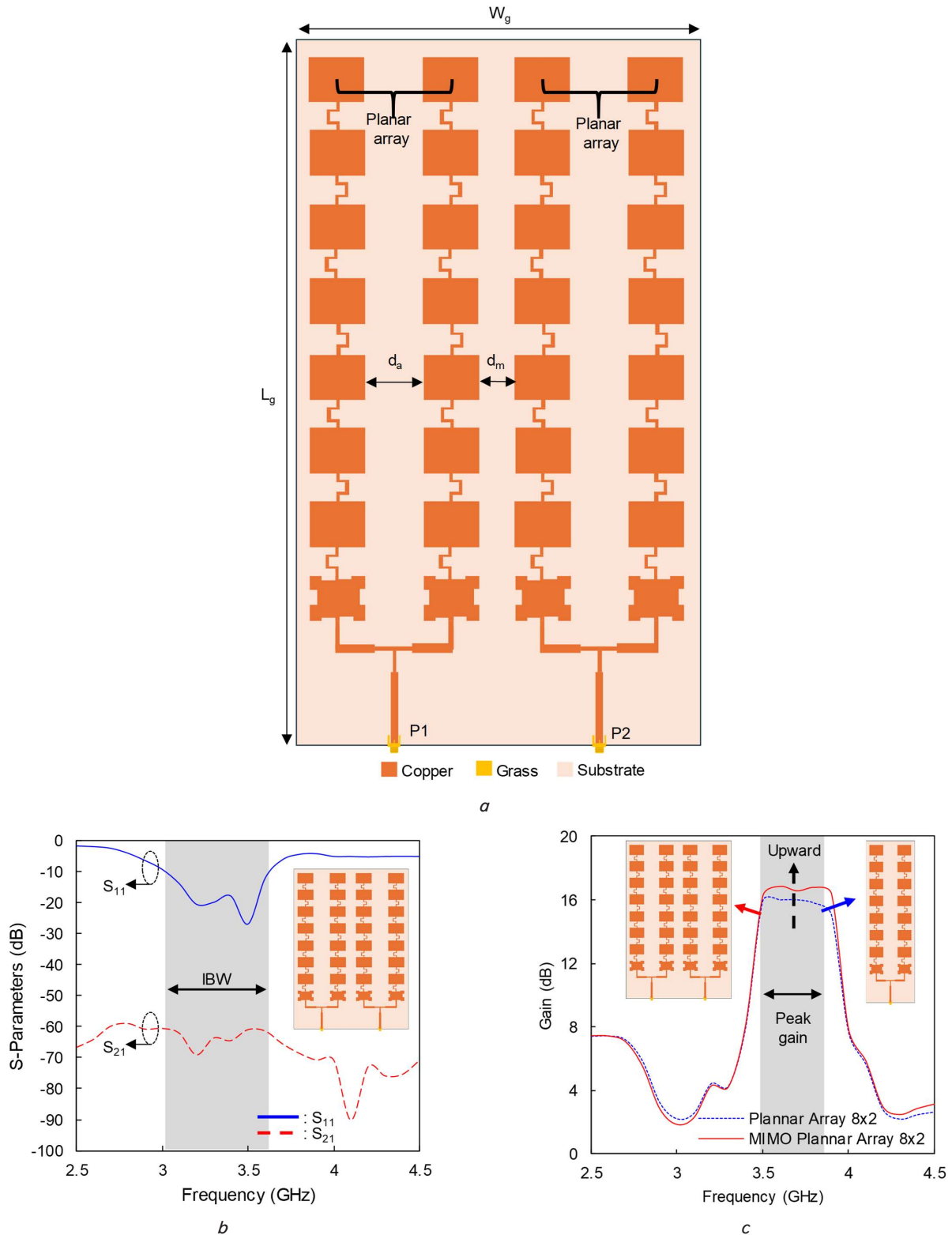

Fig. 8. Model of a MIMO series planar array antenna: a — design of an 8×2 element MIMO planar array; b — simulation of S_{11}; c — simulation of VSWR; d — simulation of gain

The next step is to optimize the antenna with a MIMO configuration that is directly connected to port 1 and port 2, respectively. It should be noted that the distance between the antennas at each port greatly affects the mutual coupling of the MIMO configuration. Mutual coupling shows the independence of the antennas when both works simultaneously. The minimum standard for mutual coupling is $S_{21} \leq -20$ dB at the specified resonant frequency.

Furthermore, to support the 5G communication system, the antenna is configured in MIMO with 2 different ports represented by port 1 (P1) and port 2 (P2) as shown in Fig. 8, a. The structure of the series planar antenna array is connected to P1 and P2, respectively. In order to control the independence of the two antennas with high mutual coupling, the antennas are separated by a certain distance represented by d_m=21 mm. The dimensions of the ground plane are represented by W_g and L_g, which are 164 mm and 353 mm, respectively.

The simulation results illustrated in Fig. 8, b show that the antenna has been operating at a resonant frequency of 3.5 GHz with S_{11} and S_{21} around -20 dB and -60 dB with a bandwidth of 650 MH (3–3.65 GHz). This finding indicates that the antenna has a bandwidth that meets the criteria for the 5G communication system and has high mutual coupling with $S_{21} \leq -20$ dB. In addition, the gain of the antenna with MIMO configuration also increases from 15.98 dB to 16.78 dB as shown in Fig. 8, c. This shows that the proposed antenna has met the specifications for 5G communication systems where the gain is ≥ 12 dB. The next stage is to fabricate and validate the performance of the proposed antenna through a measurement process in the laboratory.

5. 3. Validation and measurement of the proposed antenna

The antenna is fabricated using an FR-4 substrate where the radiating element is located on the top layer while the bottom layer functions as a ground plane as shown in Fig. 9, c. Validation of the near-field performance is carried out through a measurement process using a Vector Network Analyzer (VNA) with a frequency range of 2.5–4.5 GHz, a frequency step size of 0.01 GHz and a temperature of 25°, which is connected to the antenna (AUT) via port 1 and port 2 with a coaxial cable as shown in Fig. 9, a.

The measurement setup consists of an antenna under test (AUT), which functions as a transmitter (Tx) connected to an RF generator while a reference antenna is placed as a receiver (Rx) connected to a spectrum analyzer and separated based on the Fresnel zone where d_f=2D^2/λ [20]. The antenna is placed on a rotator that rotates clockwise from 0–360° with a step size of 1°. The far-field characteristics of the proposed antenna are observed based on the antenna's radiation pattern when transmitting and receiving electromagnetic waves.

A comparison of the simulation and measurement results of S_{11} and S_{21} in Fig. 10, a show that the fabricated antenna has the same performance as the simulated antenna where S_{11} is around -20 dB while S_{21} is around -40 dB at a resonance frequency of 3.5 GHz. The bandwidth of the fabricated antenna is 680 MHz with a frequency range

of 3–3.68 GHz. This finding shows that the measurement results are in line with the simulation results.
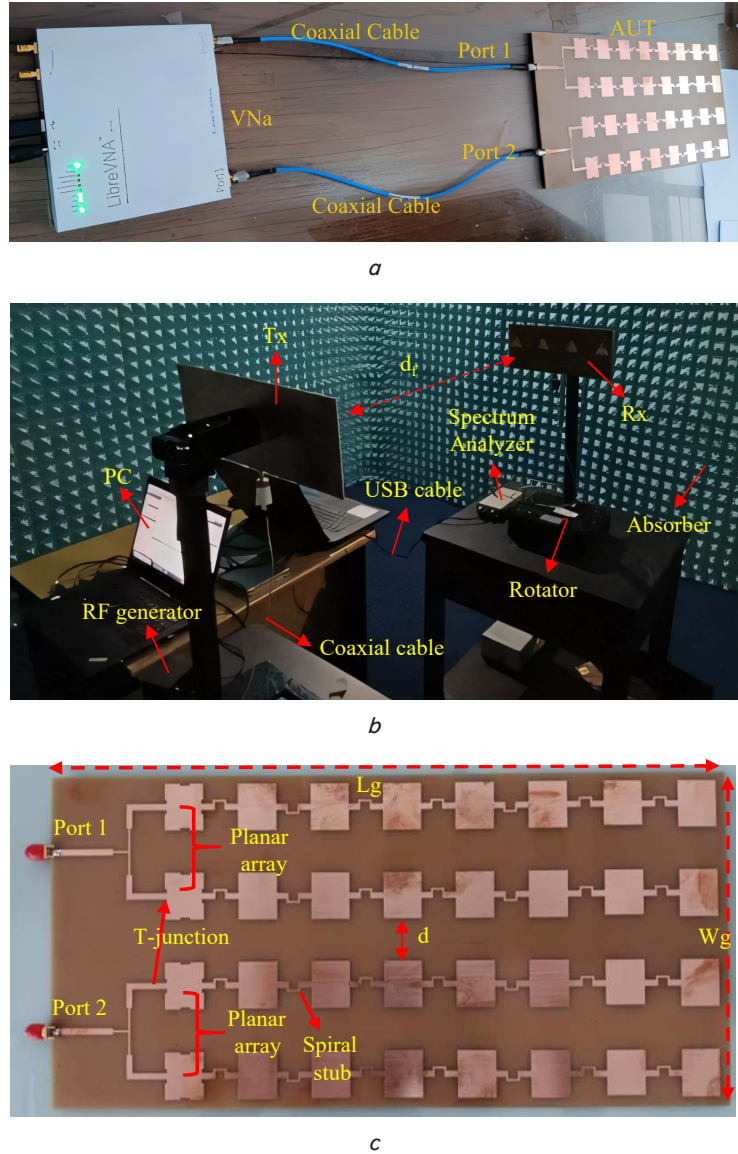
a

b

c

Fig. 9. Measurement process of the proposed antenna:
a — measurement setup for near-field validation;
b — measurement setup for far-field validation in an anechoic chamber;
c — fabrication of the proposed antenna

The subsequent phase involves assessing the performance of the MIMO antenna by examining the Envelope Correlation Coefficient (ECC) and Diversity Gain (DG) parameters. The ECC quantifies the correlation between the two antennas operating in tandem within a MIMO configuration. Typically, the ECC value lies within the range of 0 to 1, with a threshold of ≤ 0.5 generally accepted for MIMO antenna designs. The ECC can be calculated using the following equation [20]:

$$ECC = \frac{\left| S_{11}^* S_{12} + S_{21}^* S_{22} \right|^2}{\left(1 - |S_{11}|^2 - |S_{21}|^2\right) - \left(1 - |S_{22}|^2 - |S_{12}|^2\right)}. \qquad (12)$$

Diversity Gain (DG) characterizes the capability of an antenna system to mitigate the effects of multipath fading.

The DG value reflects the system's ability to enhance or sustain the signal quality relative to noise by combining signals from multiple antennas rather than relying on a single antenna. For MIMO antennas, the diversity is typically represented by a DG value of ≤10 dB [18]. The DG can be calculated using the following equation [20]:

$$DG = 10\sqrt{1-(ECC)^2}. \tag{13}$$

Fig. 10, *b* shows that the fabricated antenna has ECC and DG of about $0-0.001$ dB and $9.99-10$ dB in the resonant frequency range of $2.5-4.5$ GHz. This finding indicates that the proposed antenna has high independence and diversity. Additionally, high diversity gain contributes to better data throughput and coverage, making the antenna system more efficient in delivering consistent performance in challenging conditions, such as urban environments or areas with obstacles.

To validate the independence and mutual coupling of the proposed antenna, a comprehensive observation of the electric field concentration by EM simulation is proposed as shown in Fig. 11, *a*. The electric field of the proposed antenna is observed at a resonant frequency of 3.5 GHz and shows that the resulting mutual coupling is low as indicated by the highest electric field only at the antenna at port 1 (P1) and does not distribute the electric field to the antenna at port 2 (P2).

Furthermore, the beamforming of the proposed antenna is shown in Fig. 11, *b* where the main lobe radiates electromagnetic waves to the front of the antenna while the side lobes radiate to the top, bottom and back of the antenna. Furthermore, the radiation pattern of the simulation and measurement process illustrated in Fig. 11, *c* shows a straight and similar result where the maximum radiation is at an angle of 0 with a transmit power of about 17.8 dB. This finding indicates that the proposed antenna has operated optimally at a resonance frequency of 3.5 GHz and supports MIMO for 5G communication systems. Moreover, a comparison of bandwidth and gain for the development models of the proposed antenna is shown in Tables 1, 2.

The bandwidth and gain enhancement of the antenna can be determined using the following equation:

$$BW = \frac{(Optimized\ BW - Initial\ BW)}{Initial\ BW} \times 100\%, \tag{14}$$

$$Gain = \frac{(Optimized\ Gain - Initial\ Gain)}{Initial\ Gain} \times 100\%. \tag{15}$$

Table 1

Comparison of bandwidth for the proposed antenna models

Model	Frequency range (GHz)	Bandwidth (MHz)
1st model	3.48–3.52	40
2nd model	3.2–3.6	400
3rd model	3.3–3.6	300
4th model	3.3–3.6	300
5th model	3–3.6	600
6th model	3–3.65	650

Table 2

Comparison of gain for the proposed antenna models

Model	Frequency range (GHz)	Gain (dB)
1st model	3.48–3.52	5.8
2nd model	3.2–3.6	7.82
3rd model	3.3–3.6	9.9
4th model	3.3–3.6	10.8
5th model	3–3.6	16.09
6th model	3–3.65	17.8

Based on equation (14) and equation (15), the increase in gain and bandwidth is obtained by calculating the difference between the bandwidth and gain of the antenna with the initial condition and the optimized condition. In this study, the initial bandwidth and gain used are single-element antennas while the bandwidth and optimization gain are obtained from MIMO array antennas with 8×2 elements.
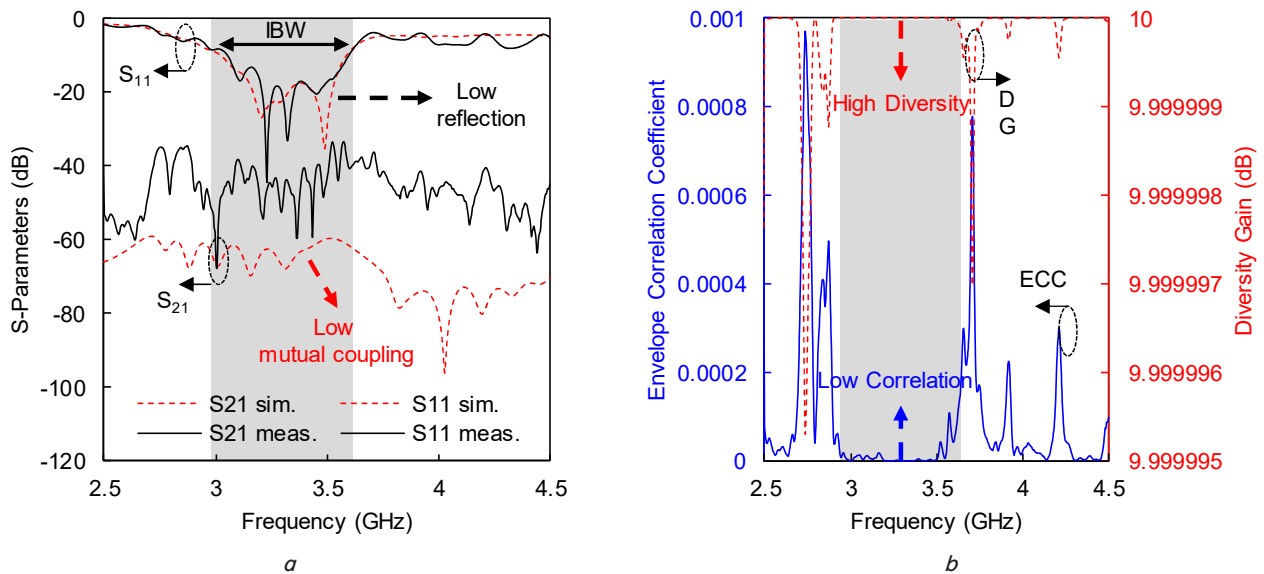

Fig. 10. Performance of the proposed antenna: *a* — comparison of the simulation and measurement results of S_{11} and S_{21}; *b* — envelope correlation coefficient and diversity gain based on measurement results
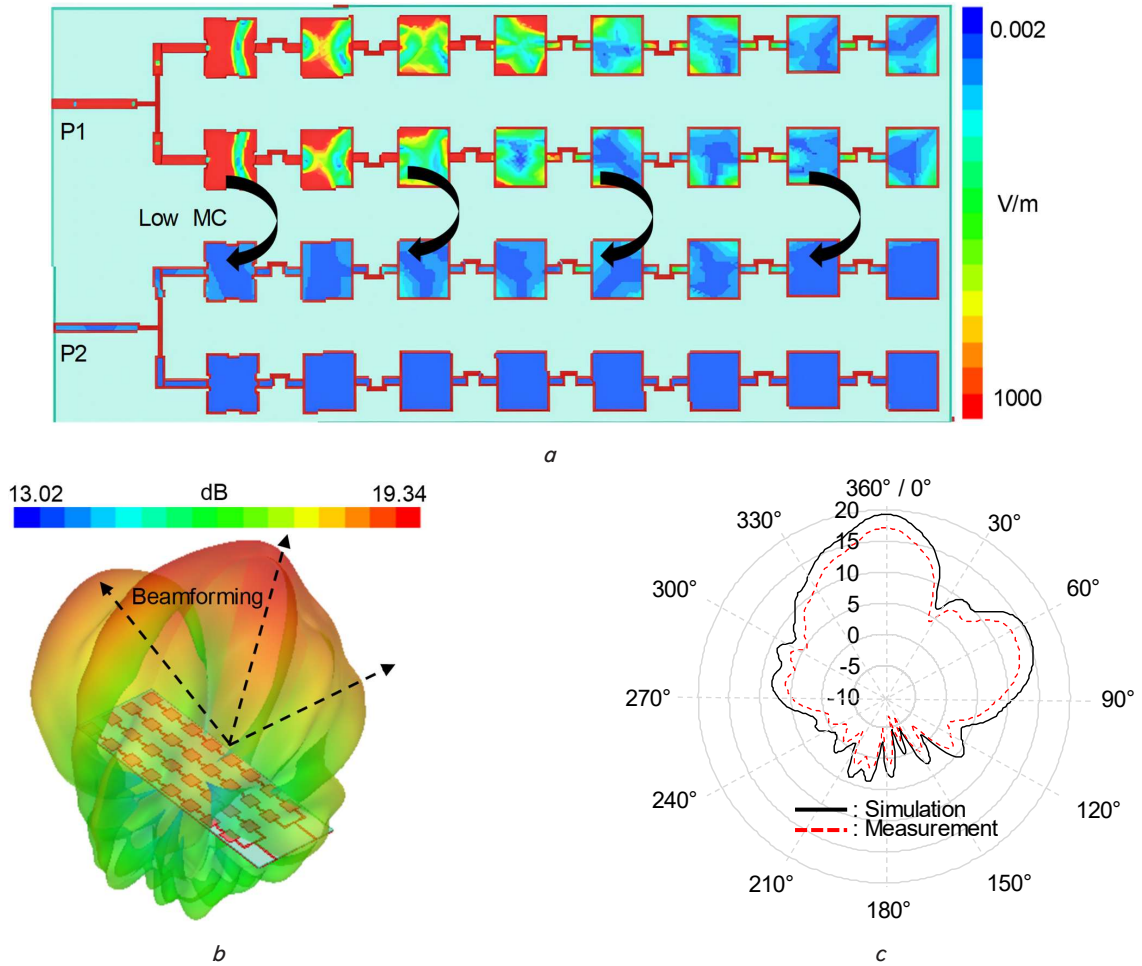
Fig. 11. MIMO performance of the proposed antenna: *a* — simulation of the E-field concentration of the proposed antenna at f_r=3.5 GHz; *b* — 3D simulation of the radiation of the proposed antenna at f_r=3.5 GHz; *c* — comparison of the simulation and measurement of the radiation pattern at f_r=3.5 GHz

6. Discussion of performance validation of the proposed MIMO antenna

Based on the measurement process, the comparison of the bandwidth of all the proposed antenna models is shown in Table 1. Based on Table 1, the bandwidth of the antenna with model 1 increases significantly from 40 MHz to 400 MHz in model 2 and 300 MHz in models 3 and 4. Furthermore, in models 5 and 6, the bandwidth increases to 600 MHz and 650 MHz. From the measurement results, it is found that the bandwidth of the antenna increases up to 1,525 % compared to the single-element antenna.

Furthermore, evaluation is also done by observing the gain of the proposed antenna. The gain comparison of the entire antenna model is shown in Table 2. Based on Table 2, the antenna gains increase in line with the addition of the number of elements of the antenna array. In model 1, the antenna gain is 5.8 dB while for model 2, model 3 and model 4, the antenna gains increase to 7.8 dB, 9.9 dB and 10.2 dB, respectively. Furthermore, in model 5 and model 6, the antenna gains increase to 16.09 and 17.8 dB.

Overall, the gain of the antenna increases up to 206.8 % compared to the single-element antenna. This finding shows that the evolution of the antenna has successfully improved the antenna performance by producing high gain. In addition, the MIMO performance of the antenna is shown with

high mutual coupling $S_{21} \le -20$ dB. From the measurement results, a mutual coupling S_{21} of −40 dB was obtained in the frequency range of 2.5 4.5 GHz. MIMO performance is also indicated by high diversity with a diversity gain of 9.9 dB and a low correlation of 0.0001. This finding shows that the antennas have high independence and do not affect each other when working together.

From the results obtained, the proposed antenna has a performance with wide bandwidth and high gain compared to previous works [15–18]. In addition, the proposed antenna also has the capability for a high-performance MIMO system compared to the previous work [19], which proposed an antenna for a 5G communication system that does not support MIMO systems.

However, there are certain limitations, such as the relatively large antenna dimensions and its operation being restricted to a single resonant frequency. Consequently, future research efforts will focus on minimizing the antenna's dimensions and enhancing its performance across multiple resonant frequencies, enabling its application in other communication systems like 4G, Zigbee, and Wi-Fi.

7. Conclusions

1. From the measurement results, it was found that the proposed antenna has operated at a frequency of 3.5 GHz

with a wide bandwidth of 680 MHz. The bandwidth of the antenna has successfully met the standard requirements for a 5G communication system where the minimum bandwidth is ≤200 MHz.

2. The gain of the proposed antenna was successfully increased gradually using a series planar array with 8×2 elements. From the measurement results, a gain of 17.8 dB was obtained. This finding indicates that the proposed antenna has met the target with a gain of ≥12 dB for a 5G communication system.

3. The proposed antenna has been successfully developed with a two-port MIMO configuration operating at a resonant frequency of 3.5 GHz. From the measurement results, it was found that the proposed antenna has a high mutual coupling with S_{21} of −40 dB with ECC 0.001 and DG 9.99 dB. This finding indicates that the proposed antenna has met the criteria of high mutual coupling with $S_{21} \leq −20$ dB.

Conflict of interest

The authors declare that they have no conflict of interest in relation to this research, whether financial, personal, authorship or otherwise, that could affect the research, and its results presented in this paper.

Data availability

The manuscript has no associated data.

Use of artificial intelligence

The authors confirm that they did not use artificial intelligence technologies when creating the current work.

References

1. Kamal, S., Bin Ain, M. F., Ullah, U., Mohammed, A. S. B., Najmi, F., Hussin, R. et al. (2021). Wheel-shaped miniature assembly of circularly polarized wideband microstrip antenna for 5G mmWave terminals. Alexandria Engineering Journal, 60 (2), 2457–2470. https://doi.org/10.1016/j.aej.2020.12.054

2. Fante, K. A., Gemeda, M. T. (2021). Broadband microstrip patch antenna at 28 GHz for 5G wireless applications. International Journal of Electrical and Computer Engineering (IJECE), 11 (3), 2238. https://doi.org/10.11591/ijece.v11i3.pp2238-2244

3. Tarpara, N., Rathwa, R. R., Kotak, D. N. A. (2018). Design of Slotted Microstrip patch Antenna for 5G Application. Int. Res. J. Eng. Technol., 5 (4), 2827–2832.

4. Hussain, R., Alreshaid, A. T., Podilchak, S. K., Sharawi, M. S. (2017). Compact 4G MIMO antenna integrated with a 5G array for current and future mobile handsets. IET Microwaves, Antennas & Propagation, 11 (2), 271–279. https://doi.org/10.1049/iet-map.2016.0738

5. Deng, J., Li, J., Zhao, L., Guo, L. (2017). A Dual-Band Inverted-F MIMO Antenna With Enhanced Isolation for WLAN Applications. IEEE Antennas and Wireless Propagation Letters, 16, 2270–2273. https://doi.org/10.1109/lawp.2017.2713986

6. Ojaroudi Parchin, N., Jahanbakhsh Basherlou, H., Al-Yasir, Y. I. A., Ullah, A., Abd-Alhameed, R. A., Noras, J. M. (2019). Multi-Band MIMO Antenna Design with User-Impact Investigation for 4G and 5G Mobile Terminals. Sensors, 19 (3), 456. https://doi.org/10.3390/s19030456

7. Hikmaturokhman, A., Ramli, K., Suryanegara, M. (2018). Spectrum Considerations for 5G in Indonesia. 2018 International Conference on ICT for Rural Development (IC-ICTRuDev). https://doi.org/10.1109/icictr.2018.8706874

8. Hobbs, S. (2018). Valuing 5G Spectrum: Valuing the 3.5 GHz and C-Band Frequency Range. Coleago Consulting.

9. An, W., Li, Y., Fu, H., Ma, J., Chen, W., Feng, B. (2018). Low-Profile and Wideband Microstrip Antenna With Stable Gain for 5G Wireless Applications. IEEE Antennas and Wireless Propagation Letters, 17 (4), 621–624. https://doi.org/10.1109/lawp.2018.2806369

10. Pratiwi, A. R., Setijadi, E., Hendrantoro, G. (2020). Design of Two-Elements Subarray with Parasitic Patch for 5G Application. 2020 International Seminar on Intelligent Technology and Its Applications (ISITIA), 7, 311–316. https://doi.org/10.1109/isitia49792.2020.9163785

11. Tang, X., Jiao, Y., Li, H., Zong, W., Yao, Z., Shan, F. et al. (2019). Ultra-Wideband Patch Antenna for Sub-6 GHz 5G Communications. 2019 International Workshop on Electromagnetics: Applications and Student Innovation Competition (IWEM). https://doi.org/10.1109/iwem.2019.8887933

12. Murugan, S. (2021). Compact MIMO Shorted Microstrip Antenna for 5G Applications. International Journal of Wireless and Microwave Technologies, 11 (1), 22–27. https://doi.org/10.5815/ijwmt.2021.01.03

13. Naik, P. S., Virani, H. G. (2020). 1×4 Microstrip Patch Slotted Array Antenna for 5G C-Band Access Point Application. 2020 International Conference on Electronics and Sustainable Communication Systems (ICESC), 1, 641–644. https://doi.org/10.1109/icesc48915.2020.9156015

14. Aghoutane, B., Das, S., EL Ghzaoui, M., Madhav, B. T. P., El Faylali, H. (2022). A novel dual band high gain 4-port millimeter wave MIMO antenna array for 28/37 GHz 5G applications. AEU - International Journal of Electronics and Communications, 145, 154071. https://doi.org/10.1016/j.aeue.2021.154071

15. Naga Jyothi Sree, G., Nelaturi, S. (2021). Design and experimental verification of fractal based MIMO antenna for lower sub 6-GHz 5G applications. AEU - International Journal of Electronics and Communications, 137, 153797. https://doi.org/10.1016/j.aeue.2021.153797

16. Hu, W., Liu, X., Gao, S., Wen, L.-H., Qian, L., Feng, T. et al. (2019). Dual-Band Ten-Element MIMO Array Based on Dual-Mode IFAs for 5G Terminal Applications. IEEE Access, 7, 178476–178485. https://doi.org/10.1109/access.2019.2958745

17. Xu, K. D., Zhu, J., Liao, S., Xue, Q. (2018). Wideband Patch Antenna Using Multiple Parasitic Patches and Its Array Application With Mutual Coupling Reduction. IEEE Access, 6, 42497–42506. https://doi.org/10.1109/access.2018.2860594

18. Alam, S., Surjati, I, Sari, L., Anindito, A., Putranto, A. Y., Firmansyah, T. (2021). Bandwidth Enhancement of Array Microstrip Antenna Using Spiral Stub For 5G Communication System. PRZEGLĄD ELEKTROTECHNICZNY, 1 (11), 42–46. https://doi.org/10.15199/48.2021.11.07

19. Alam, S., Surjati, I., Sari, L., Ningsih, Y. K., Suryadi, S., Trihantoro, G. et al. (2023). Wide band and high gain microstrip antenna using planar series array 4×2 element for 5G communication system. Eastern-European Journal of Enterprise Technologies, 4 (5 (124)), 16–24. https://doi.org/10.15587/1729-4061.2023.285395

20. Putri, S., Surjati, I., Alam, S., Ningsih, Y. K., Sari, L., Firmansyah, T., Zakaria, Z. (2024). High Isolation of Dual-Band MIMO Microstrip Antenna with Vertical – Horizontal Configuration for 5G Communication System. PRZEGLĄD ELEKTROTECHNICZNY, 1 (4), 89–95. https://doi.org/10.15199/48.2024.04.17

21. Fang, D. G. (2017). Antenna Theory and Microstrip Antennas. CRC Press. https://doi.org/10.1201/b10302

22. Garg, R., Bhartia, P., Bahl, I. J., Ittipiboon, A. (2001). Microstrip antenna design handbook. ARTECH HOUSE. Available at: https://uodiyala.edu.iq/uploads/PDF%20ELIBRARY%20UODIYALA/EL37/Microstrip%20Antenna%20Design%20Handbook.pdf